City Research Online

City St George's, University of London

Citation: Banerjee, J. R. & Ananthapuvirajah, A. (2019). An exact dynamic stiffness matrix for a beam incorporating Rayleigh–Love and Timoshenko theories. International Journal of Mechanical Sciences, 150, pp. 337-347. doi: 10.1016/j.ijmecsci.2018.10.012

This is the accepted version of the paper.

This version of the publication may differ from the final published version. To cite this item please consult the publisher's version.

Permanent repository link: https://openaccess.city.ac.uk/id/eprint/20916/

Link to published version: https://doi.org/10.1016/j.ijmecsci.2018.10.012

Copyright and Reuse: Copyright and Moral Rights remain with the author(s) and/or copyright holders. Copies of full items can be used for personal research or study, educational, or not-for-profit purposes without prior permission or charge, unless otherwise indicated, provided that the authors, title and full bibliographic details are credited, a hyperlink and/or URL is given for the original metadata page and the content is not changed in any way. For full details of reuse please refer to City Research Online policy.

City Research Online: http://openaccess.city.ac.uk/ publications@citystgeorges.ac.uk

AN EXACT DYNAMIC STIFFNESS MATRIX FOR A BEAM INCORPORATING RAYLEIGH-LOVE AND TIMOSHENKO THEORIES

J.R. Banerjee and A. Ananthapuvirajah

Department of Mechanical Engineering and Aeronautics
School of Mathematics, Computer Science and Engineering
City, University of London, Northampton Square, London EC1V 0HB

ABSTRACT

An exact dynamic stiffness matrix for a beam is developed by integrating the Rayleigh-Love theory for longitudinal vibration into the Timoshenko theory for bending vibration. In the formulation, the Rayleigh-Love theory accounted for the transverse inertia in longitudinal vibration whereas the Timoshenko beam theory accounted for the effects of shear deformation and rotating inertia in bending vibration. The dynamic stiffness matrix is developed by solving the governing differential equations of motion in free vibration of a Rayleigh-Love bar and a Timoshenko beam and then imposing the boundary conditions for displacements and forces. Next the two dynamic stiffness theories are combined using a unified notation. The ensuing dynamic stiffness matrix is subsequently used for free vibration analysis of uniform and stepped bars as well as frameworks through the application of the Wittrick-Williams algorithm as solution technique. Illustrative examples are given to demonstrate the usefulness of the theory and some of the computed results are compared with published ones. The paper closes with some concluding remarks.

Keywords: Rayleigh-Love bar; Timoshenko beam; dynamic stiffness method; Wittrick-Williams algorithm.

*Corresponding author.
Email address: j.r.banerjee@city.ac.uk

1. Introduction

Free vibration analysis in the high frequency range is of great importance to assess the flow of vibrational energy in structures, particularly when the widely accepted Statistical Energy Analysis (SEA) method [1, 2] is used. Research in this area is further motivated by the fact that the modal density required for the energy flow analysis in structures is generally very high in the high frequency range. To this end there are several research papers in the published literature on the energy flow analysis in classical structures such as bars [3], beams [4], membranes [5] and plates [6] which emphasize the need for high frequency vibration analysis. For accurate and efficient high frequency vibration analysis, these publications highlight the inadequacy of the traditional finite element method (FEM) which is somehow limited to low and perhaps medium frequency range unless high-precision, good quality finite elements are used which may become computationally very expensive. In the particular context of free vibration of beams, there are numerous books on mechanical vibration [7-11] which give the natural frequencies and mode shapes in longitudinal, torsional and bending vibration through the solution of the governing differential equations and imposition of the boundary conditions to eliminate the integration constants which eventually lead to the frequency equation. This standard and relatively simple procedure is straightforwardly taught in most of the undergraduate engineering curriculum across the globe. As the classical results of the free vibration analysis come from the solution of the governing differential equation, they are generally considered to be exact. Similar and comparable, but somehow approximate results for beam vibration problems can also be obtained by applying the FEM which requires discretisation of the beam into several elements and assembling the element stiffness and mass matrices which ultimately lead to a linear eigenvalue formulation. Clearly the order of the mass and stiffness matrices in the FEM decides the number of natural frequencies that can be meaningfully computed. The higher order natural frequencies and mode shapes will, of course, be considerably less accurate. At this point it should be noted that there is a powerful alternative to FEM as well the classical method, which has no restriction on higher order natural frequency computation and yet it retains the exactness of results. The alternative is that of the dynamic stiffness method (DSM) which is elegant and versatile and hence can be used in a much broader context to analyse the free vibration behaviour of complex structures. The DSM is different, but in many ways similar to the FEM in that it has analogous procedure for assembling structural properties of individual structural elements. However, a major difference exists

between the DSM and the FEM which is that the former is unaffected by the number of elements used in the analysis and always gives exact results whereas the latter is mesh dependent and the accuracy of results depends on the number of elements used in the analysis. For instance, one single structural element can used in the DSM to compute any number of natural frequencies without any loss of accuracy which, of course, is impossible in the FEM. The DSM was pioneered by Kolousek [12-14] in the early 1940s and it has since been used to investigate the free vibration behaviour of beams and frameworks in an exact sense [15-17]. The uncompromising accuracy of the DSM stems from the fact that the frequency dependent shape function used to derive the element dynamic stiffness matrix of a structural element comes from the exact solution of the governing differential equation of motion of the element undergoing free natural vibration. The element dynamic stiffness matrix derived in this way contains both the mass and stiffness properties of the element, unlike the FEM for which the mass and stiffness matrices are always separate and frequency independent, and they are generally derived from assumed shape functions. An outline for the procedure to derive the dynamic stiffness matrix of a structural element can be found in the work of Banerjee [18]. The overall frequency dependent dynamic stiffness matrix of the final structure is obtained by assembling the individual dynamic stiffness matrices of all constituent elements in the structure, in the usual way as in the case of the FEM, but the formulation leads to a non-linear eigenvalue problem and the natural frequencies are generally extracted by applying the well-established algorithm of Wittrick and William [19]. Because of the independency of the accuracy of results on the number of element used in the analysis, the DSM is ideally suited for free vibration analysis in all frequency ranges.

Following the work of Kolousek [12-14], the DSM has been implemented in computer programs published by Akesson [15], Williams and Howson [16] and Howson et al [17] to investigate the free vibration characteristics of plane frames, which required the dynamic stiffness matrices of both bar and beam elements as building blocks. The bar theory accounts for the axial stiffness and the beam theory accounts for the bending stiffness. As the coupling between them is generally ignored, the dynamic stiffness matrix of the element used to investigate the free vibration behaviour of plane frames [15-17] was obtained by separate consideration of axial and bending deformation and then combining the two together in matrix form. In these earlier works, when the axial stiffnesses were incorporated into the bending stiffnesses to construct the dynamic stiffness matrix of an individual element, only classical theory for longitudinal free vibration of bars which ignores the transverse inertia effect was

used. This is generally justified, particularly in the low and probably in the medium frequency range, but for high frequency vibration, the so-called Rayleigh-Love theory [20, 21] which accounts for the effects of transverse inertia during longitudinal vibration and the Timoshenko theory [17] which accounts for the effects of shear deformation and rotatory inertia during bending vibration need to be considered. This is particularly important when applying the widely accepted SEA technique for which the high frequency vibration problem must be modelled properly [1-2]. In this respect, the traditional FEM may become inaccurate.

From a historical perspective, it was Lord Rayleigh [22] who first recognised the importance of transverse inertia on the longitudinal free vibration of bars, particularly at high frequencies. Many years later, Love [23] shed further lights on Lord Rayleigh's work which eventually took the name Rayleigh-Love theory and the research took significant turn to wave propagation and vibrational energy analysis [24-26] of bars in longitudinal motion. No one appears to have made any attempt to combine the Rayleigh-Love bar analysis with flexure, particularly when investigating the free vibration characteristics of frameworks. This will be important within the high frequency range when using the SEA technique. The purpose of this paper is to fill this gap in the literature. First, the dynamic stiffness matrix of a Rayleigh-Love bar is developed from the fundamental equation of motion in longitudinal free vibration. Then the developed dynamic stiffness matrix of the Rayleigh-Love bar is integrated with the dynamic stiffness matrix of a Timoshenko beam [27-30] which accounts for the effects of shear deformation and rotatory inertia to allow for the free vibration analysis of individual members and plane frames in the low, medium and high frequency range through the application of the Wittrick-Williams algorithm [19] as solution technique. Using the developed theory, a wide range of problems is solved and some of the computed results are compared with published literature. The paper draws significant conclusions on the effects of the inclusion of transverse inertia arising from the Rayleigh-Love theory and shear deformation and rotatory inertia from the Timoshenko theory when investigating the free vibration characteristics of individual members, stepped members as well as frameworks.

It should be noted that there are no specific hard boundaries between the regimes of low, medium and high frequencies, but a useful descriptor which gives an indicative guidance to frequency range is the vibrational wavelength when compared to the overall length of the structure. Thus an engineering judgement can be reasonably made based on the product of the wave number and a typical length of the structure, which is essentially the Helmholtz number. Large values of this number represent the high frequency range whereas lower values

determine the low to medium frequency range. For the type of problems investigated in this paper, the low to medium range of frequencies is characterised to be below 1500 HZ whereas frequencies above this value constitute the high frequency range.

2. Dynamic Stiffness Formulation

The dynamic stiffness matrix of a structural element essentially relates the amplitudes of the forces to those of the corresponding displacements at the nodes of the harmonically vibrating structural element. A general procedure to formulate the dynamic stiffness matrix of a structural element is briefly described in following steps:

(i) Derive the governing differential equation of motion in free vibration of the structural element for which the dynamic stiffness matrix is to be developed. This can be achieved by applying Newton's second law or Lagrange's equation or Hamilton's principle. However, Hamilton's principle is preferred because unlike Newton's second law and Lagrange's equation, the variationally based Hamilton's principle provides natural boundary conditions, giving the expressions for forces and moments which are required in the dynamic stiffness formulation.

(ii) For harmonic oscillation, seek a closed form analytical solution of the governing differential equation derived in (i) above, in terms of the arbitrary integration constants. The number of constants in the general solution will, of course, depend on the order of the differential equation.

(iii) Apply the boundary conditions in algebraic form. The number of boundary conditions is generally equal to twice the number of integration constants. The boundary conditions are typically the nodal displacements and forces.

(iv) Eliminate the constants by relating the harmonically varying amplitudes of nodal forces to the corresponding displacements at the nodes of the element. This will generate the frequency dependent dynamic stiffness matrix connecting dynamically the amplitudes of the nodal forces to those of the nodal displacements.

The axial deformation of a Rayleigh-Love bar and the bending deformations of a Timoshenko beam are considered uncoupled and treated independently so that the derivation of the dynamic stiffness matrix for each of them can be carried out separately, and later integrated.

2.1 Dynamic Stiffness Matrix of a Rayleigh-Love Bar

A uniform Rayleigh-Love bar of length L is shown in Fig. 1 in a rectangular right handed Cartesian co-ordinate system with the X-axis coinciding with the axis of the bar. Note that Fig. 1 can also be used to represent a beam which is also a two-noded line element like a bar element. The essential difference between a bar and a beam element is that the former can sustain only axial load whereas the latter can take bending and shear load, as well as the axial load. In other words, in any local coordinate system such as the one shown in Fig. 1, a bar element can undergo only axial deformation whereas a beam element can undergo bending displacement, bending rotation as well as axial deformation. Now the governing differential equation of motion of the Rayleigh-Love bar in free axial (or longitudinal) vibration can be derived by using Hamilton's principle as the first step towards the dynamic stiffness formulation. The focus area of the derivation in this section is, of course, on the axial stiffnesses only.

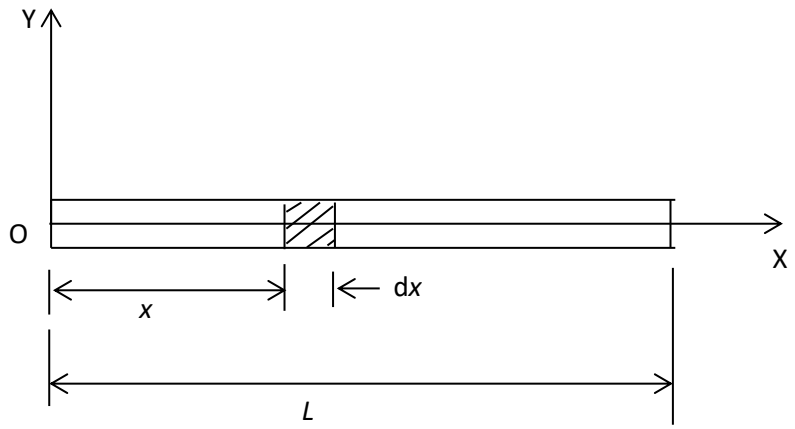

Fig. 1. Coordinate system and notation for a Rayleigh-Love bar and a Timoshenko beam.

Referring to Fig. 1 and noting that if u is the axial displacement at a distance x from the origin, the kinetic and potential energies of the bar T_{bar} and V_{bar} are respectively given by [7, 21]

$$T_{\text{bar}} = \frac{1}{2}\int_0^L \left[\rho A \left(\frac{\partial u}{\partial t}\right)^2 + \rho I_P v^2 \left(\frac{\partial^2 u}{\partial x \partial t}\right)^2\right] dx \tag{1}$$

and

$$V_{\text{bar}} = \frac{1}{2}\int_0^L EA \left(\frac{\partial u}{\partial x}\right)^2 \text{dx} \tag{2}$$

where ρ is the density of the bar material, A is the cross-sectional area of the bar so that ρA represents the mass per unit length, I_P is the polar second moment of area so that ρI_P represents the polar mass moment of inertia per unit length, E is the Young's modulus of the bar material

so that *EA* represents the axial or extensional rigidity of the bar and ν is the Poisson's ratio of the bar material.

Hamilton's principle states

$$\delta \int_{t_1}^{t_2} (T_{\text{bar}} - V_{\text{bar}})\, dt = 0 \tag{3}$$

where t_1 and t_2 are the time interval in the dynamic trajectory, and δ is the usual variational operator.

The governing differential equations of motion of the Rayleigh-Love bar and the associated boundary condition in free vibration can now be derived by substituting the kinetic (T_{bar}) and potential (V_{bar}) energy expressions of Eqs. (1) and (2) into Eq. (3), using the δ operator, integrating by parts and then collecting terms. In an earlier publication, the entire procedure to generate the governing differential equations of motion and natural boundary conditions for bar or beam type structures was automated by Banerjee et al [31] by applying symbolic computation. In this way, the governing differential equation of motion of the Rayleigh-Love bar is obtained as [7, 21]

$$EA\frac{\partial^2 u}{\partial x^2} - \rho A\frac{\partial^2 u}{\partial t^2} + \rho I_P \nu^2 \frac{\partial^4 u}{\partial x^2 \partial t^2} = 0 \tag{4}$$

As a by-product of the Hamiltonian formulation, the expression for the axial force $f(x, t)$ follows from the natural boundary condition to give [7, 21]

$$f(x,t) = -EA\frac{\partial u}{\partial x} - \rho I_P \nu^2 \frac{\partial^3 u}{\partial x \partial t^2} \tag{5}$$

If harmonic oscillation is assumed, then

$$u(x,t) = U(x)e^{i\omega t} \tag{6}$$

where ω is the angular or circular frequency, and $U(x)$ are the amplitudes of u.

Substituting Eq. (6) into Eq. (5) gives

$$(EA - \rho I_P \nu^2 \omega^2)\frac{d^2 U}{dx^2} + \rho A\omega^2 U = 0 \tag{7}$$

As a result of the harmonic oscillation assumption, the amplitude $F(x)$ of the force $f(x, t)$ in Eq. (5) becomes

$$F(x) = -(EA - \rho I_P \nu^2 \omega^2)\frac{dU}{dx} \tag{8}$$

Introducing the differential operator $D = d/d\xi$ and the non-dimensional length ξ as

$$\xi = \frac{x}{L} \tag{9}$$

Eq. (7) becomes

$$(D^2 + \gamma^2)U = 0 \tag{10}$$

where

$$\gamma^2 = \frac{\alpha^2}{1-\beta^2} \tag{11}$$

with

$$\alpha^2 = \frac{\rho A \omega^2 L^2}{EA}; \qquad \beta^2 = \frac{\rho I_P \nu^2 \omega^2}{EA} \tag{12}$$

The expression for the amplitude of the axial force in Eq. (8) using Eqs. (9) and (12) becomes

$$F(\xi) = -\frac{EA}{L}(1-\beta^2)\frac{dU}{d\xi} \tag{13}$$

The solution of the differential equation, Eq. (10) is given by

$$U(\xi) = C_1 \sin\gamma\xi + C_2 \cos\gamma\xi \tag{14}$$

where C_1 and C_2 are constants.

The expression for axial force $F(\xi)$ can now be expressed by substituting Eq. (14) into Eq. (13) to give

$$F(x) = F(\xi) = -\frac{EA}{L}(1-\beta^2)\gamma(C_1 \cos\gamma\xi - C_2 \sin\gamma\xi) \tag{15}$$

Now referring to Fig. 2, the boundary conditions for displacements and forces can be applied as follows.

At $x = 0$ (i.e. $\xi = 0$), $U = \Delta_{x1}$ and $F = F_{x1}$ (16)

At $x=L$ (i.e. $\xi = 1$), $U = \Delta_{x2}$ and $F = -F_{x2}$ (17)

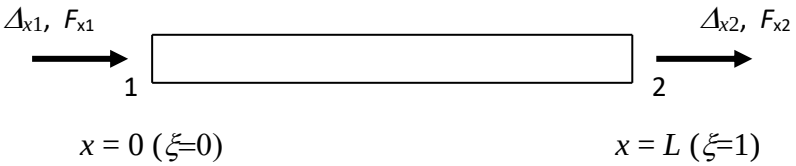

Fig. 2. Boundary conditions for displacements and forces in axial vibration for a Rayleigh-Love bar

Substituting Eqs. (16) and (17) into Eqs. (14) and (15), the following matrix relationships can be obtained

$$\begin{bmatrix}\Delta_{x1}\\ \Delta_{x2}\end{bmatrix} = \begin{bmatrix}0 & 1\\ \sin\gamma & \cos\gamma\end{bmatrix}\begin{bmatrix}C_1\\ C_2\end{bmatrix} \tag{18}$$

and

$$\begin{bmatrix} F_{x1} \\ F_{x2} \end{bmatrix} = \frac{EA}{L}\gamma(1-\beta^2)\begin{bmatrix} -1 & 0 \\ \cos\gamma & -\sin\gamma \end{bmatrix}\begin{bmatrix} C_1 \\ C_2 \end{bmatrix} \tag{19}$$

The constants C_1 and C_2 can now be eliminated from Eqs. (18) and (19) to give the dynamic stiffness matrix of an axially vibrating Rayleigh-Love bar relating amplitudes of the forces and displacements at its ends as follows:

$$\begin{bmatrix} F_{x1} \\ F_{x2} \end{bmatrix} = \begin{bmatrix} a_1 & a_2 \\ a_2 & a_1 \end{bmatrix}\begin{bmatrix} \Delta_{x1} \\ \Delta_{x2} \end{bmatrix} \tag{20}$$

where the elements of the 2×2 dynamic stiffness matrix are given by

$$a_1 = \frac{EA}{L}\gamma(1-\beta^2)\cot\gamma\,, \qquad a_2 = -\frac{EA}{L}\gamma(1-\beta^2)\operatorname{cosec}\gamma \tag{21}$$

It should be noted that the Rayleigh-Love theory has a limitation that β^2 in Eqs. (11) and (12) must be less than one which is usually the case, otherwise, the solution of Eq. (10) would not be harmonic and hence no oscillatory motion will take place. This limitation has been pointed out in the literature, e.g. see Eq. (13) of [32].

2.2 Dynamic Stiffness Matrix of a Timoshenko Beam

The dynamic stiffness matrix of a Timoshenko beam has already been published in the literature [27-30] in a rather longwinded and complicated manner, the details of which are not repeated here. However, for clarity, completeness and importantly to make this paper self-contained, the existing literature is concisely congregated and simplified. The procedure is briefly summarised below.

Considering Fig. 1 to be the Timoshenko beam under investigation with bending rigidity EI, mass per unit length ρA and length L, undergoing bending displacement w and bending rotation θ, the expressions for kinetic and potential energies T_{beam} and V_{beam} are respectively given by [33]

$$T_{\text{beam}} = \frac{1}{2}\int_0^L \rho A\left(\frac{\partial w}{\partial t}\right)^2 dx + \frac{1}{2}\int_0^L \rho I\left(\frac{\partial \theta}{\partial t}\right)^2 dx \tag{22}$$

$$V_{\text{beam}} = \frac{1}{2}\int_0^L EI\left(\frac{\partial \theta}{\partial x}\right)^2 dx + \frac{1}{2}\int_0^L kAG\gamma^2\, dx \tag{23}$$

In Eqs. (22) and (23), ρI is the rotatory inertia per unit length about the bending axis, kAG is, the shear rigidity of the beam with k being the shear correction (also known as the shape factor) and γ is the angle of shear deformation which is essentially the shearing strain. It should be

noted that in the Timoshenko beam formulation the total slope $\frac{\partial w}{\partial x}$ is the sum of both bending slope θ and the slope due to shear γ [33] so that

$$\frac{\partial w}{\partial x} = \theta + \gamma \tag{24}$$

or

$$\gamma = \frac{\partial w}{\partial x} - \theta \tag{25}$$

Thus, the potential energy V_{beam} of Eq. (22) becomes

$$V_{\text{beam}} = \frac{1}{2}\int_0^L EI\left(\frac{\partial \theta}{\partial x}\right)^2 dx + \frac{1}{2}\int_0^L kAG\left(\frac{\partial w}{\partial x} - \theta\right)^2 dx \tag{26}$$

Substituting the expressions for the kinetic and potential energies T_{beam} and V_{beam} from Eqs. (22) and (26) into Hamilton's principle expressed in Eq. (3) and then integrating by parts and collecting terms yield the governing differential equations of motion and the associated boundary conditions providing the expressions for bending moment (M) and shear force (S) as follows [33].

Governing differential equations

$$-\rho A\frac{\partial^2 w}{\partial t^2} + kAG\frac{\partial}{\partial x}\left(\frac{\partial w}{\partial x} - \theta\right) = 0 \tag{27}$$

$$-\rho I\frac{\partial^2 \theta}{\partial t^2} + EI\frac{\partial^2 \theta}{\partial x^2} + kAG\left(\frac{\partial w}{\partial x} - \theta\right) \tag{28}$$

Natural boundary conditions

Shear Force: $$v = -kAG\left(\frac{\partial w}{\partial x} - \theta\right) = EI\frac{\partial^2 \theta}{\partial x^2} - \rho I\frac{\partial^2 \theta}{\partial t^2} \tag{29}$$

Bending Moment: $$m = -EI\frac{\partial \theta}{\partial x} \tag{30}$$

Introducing the non-dimensional length $\xi = x/L$ and assuming harmonic oscillation so that

$$w(x,t) = W(\xi)e^{i\omega t} \tag{31}$$

$$\theta(x,t) = \Theta(\xi)e^{i\omega t} \tag{32}$$

where $W(\xi)$ and $\Theta(\xi)$ are the amplitudes of the bending displacement and bending rotation of the harmonically vibrating Timoshenko beam.

Eqs. (27) and (28) can now be combined to give a fourth order ordinary differential equation as follows which is identically satisfied by both $W(\xi)$ and $\Theta(\xi)$

$$[D^4 + b^2(r^2 + s^2)D^2 - b^2(1 - b^2r^2s^2)]H = 0 \tag{33}$$

where

$$D = \frac{d}{d\xi} = \frac{1}{L}\frac{d}{dx} \tag{34}$$

$$b^2 = \frac{\rho A\omega^2 L^4}{EI}; \quad r^2 = \frac{I}{AL^2}; \quad s^2 = \frac{EI}{kAGL^2} \tag{35}$$

and

$$H = W \text{ or } \Theta \tag{36}$$

If a trial solution $H = e^{\lambda\xi}$ is assumed where λ is a constant, yet to be known, the auxiliary or characteristic equation of the differential Eq. (33) is given by

$$\lambda^4 + b^2(r^2 + s^2)\lambda^2 - b^2(1 - b^2r^2s^2) = 0 \tag{37}$$

Eq. (37) is quartic in λ, but quadratic in λ^2 so that

$$\lambda^2 = \frac{-b^2(r^2+s^2) \pm \sqrt{\{b^2(r^2+s^2)\}^2 + 4b^2(1-b^2r^2s^2)}}{2} = \frac{-b^2(r^2+s^2) \pm \sqrt{\{b^2(r^2-s^2)\}^2 + 4b^2}}{2} \tag{38}$$

Clearly λ^2 will be always real and for the negative value of the expression under the square root sign of Eq. (38), one of the two values of λ^2 will be always negative, resulting in two imaginary roots of λ which will lead to part of the solution of Eq. (33) in terms of trigonometric functions whereas the other value of λ^2 when using the positive value before the square root sign can be either positive or negative depending on whether the square root expression in Eq. (38) is bigger than or smaller than $b^2(r^2 + s^2)$. If this second value of λ^2 is positive which is usually the case, the two roots of λ^2 will be real, yielding the remaining solution of Eq. (33) in terms of hyperbolic functions so that the two of the four integration constants in the solution will be connected to trigonometric functions and the other two to hyperbolic functions. However, for exceptionally high frequencies or for exceptionally squat beams, the second value of λ^2 can be negative like the first one which will give the entire solution of Eq. (33) in terms of trigonometric functions only. The two sets of solutions and their conditionality are explained below.

The expression for λ^2 in Eq. (38) can be expressed in the following alternative form

$$\lambda^2 = \frac{b^2}{2}\left\{-(r^2 + s^2) \pm \sqrt{(r^2 + s^2)^2 + \frac{4}{b^2}(1 - b^2r^2s^2)}\right\} \tag{39}$$

It is clear from Eq. (39) that if $b^2r^2s^2 < 1$, one of the values of λ^2 will be negative and the other value will be positive whereas if $b^2r^2s^2 > 1$, they both will be negative. Thus the solutions for bending displacement W and bending rotation Θ for these two cases resulting from the differential equation of Eq. (33) are given by

(i) $b^2r^2s^2 < 1$

$$W(\xi) = A_1 \cos\Phi + A_2 \sin\Phi + A_3 \cosh\Lambda + A_4 \sinh\Lambda \tag{40}$$

$$\Theta(\xi) = B_1 \cos\Phi + B_2 \sin\Phi + B_3 \cosh\Lambda + B_4 \sinh\Lambda \tag{41}$$

(ii) $b^2r^2s^2 > 1$

$$W(\xi) = A_1 \cos\Phi + A_2 \sin\Phi + A_3 \cos\Lambda + A_4 \sin\Lambda \tag{42}$$

$$\Theta(\xi) = B_1 \cos\Phi + B_2 \sin\Phi + B_3 \cos\Lambda + B_4 \sin\Lambda \tag{43}$$

where

$$\Phi^2 = \frac{b^2(r^2+s^2)}{2} + \frac{b^2}{2}\sqrt{(r^2+s^2)^2 + \frac{4}{b^2}(1-b^2r^2s^2)} \tag{44}$$

and

$$j\Lambda^2 = -\frac{b^2(r^2+s^2)}{2} + \frac{b^2}{2}\sqrt{(r^2+s^2)^2 + \frac{4}{b^2}(1-b^2r^2s^2)} \tag{45}$$

with

$$j = 1 \text{ for } b^2r^2s^2 < 1\ ; \quad j = -1 \text{ for } b^2r^2s^2 > 1 \tag{46}$$

and A_1 - A_4 and B_1 - B_4 are two different sets of constants.

It should be noted from Eq. (35) that

$$b^2r^2s^2 = \frac{\rho I\omega^2}{kAG} \tag{47}$$

For most of the practical problems, $b^2r^2s^2$ will be less than one unless ω is exceptionally large. This is because the shear rigidity kAG is generally much bigger than the rotatory inertia per unit length ρI for any realistic cross-section and beam material, but nevertheless, the solutions given by Eqs. (42) and (43) are included in the theory to cover the exceptional case when $b^2r^2s^2$ is greater than one.

With the help of Eq. (27) or (28) and the solution given by Eqs. (40)-(43), it can be shown that the two sets of constants A_1 - A_4 and B_1 - B_4 are related. Using Eq. (27), the following relationships between B_1 - B_4 and A_1 - A_4 are obtained.

$$B_1 = \frac{k_\Phi}{L}A_2; \quad B_2 = -\frac{k_\Phi}{L}A_1; \quad B_3 = \frac{k_\Lambda}{L}A_4; \quad B_4 = j\frac{k_\Lambda}{L}A_3 \tag{48}$$

where

$$k_\Phi = \left(\frac{\Phi^2 - b^2s^2}{\Phi}\right); \qquad k_\Lambda = \left(\frac{\Lambda^2 + jb^2s^2}{\Lambda}\right) \tag{49}$$

Because of the harmonic oscillation hypothesis adopted for the freely vibrating Timoshenko beam as indicated by Eqs. (31) and (32) and also by the introduction of the non-dimensional length $\xi = x/L$, the expressions for the amplitudes of the shear force (V) and bending moment (M) arising from Eqs. (29), (30) and (48) will take the following form.

$$V = \frac{EI}{L^2}\left(\frac{d^2\Theta}{d\xi^2} - b^2r^2\Theta\right)$$

$$= \frac{EI}{L^3}(A_1e_\Phi \sin\Phi\xi - A_2e_\Phi \cos\Phi + jA_3e_\Lambda \sin\Lambda\xi + A_4e_\Lambda \cos\Lambda\xi) \tag{50}$$

$$M = -\frac{EI}{L^2}\frac{d\Theta}{d\xi}$$

$$= -\frac{EI}{L^2}(-A_1\Phi k_\Phi \cos\Phi\xi - A_2\,\Phi k_\Phi \sin\Phi\xi + jA_3\,\Lambda k_\Lambda \cos\Lambda\xi + jA_4\Lambda k_\Lambda \sin\Lambda\xi) \quad (51)$$

where

$$e_\Phi = (\Phi^2 - b^2r^2)k_\Phi; \qquad e_\Lambda = j(\Lambda^2 + jb^2r^2)k_\Lambda \quad (52)$$

and j and k_Φ, k_Λ have already been defined in Eqs. (46) and (49), respectively.

Now from the expressions for the amplitudes of displacements W and Θ given by Eqs. (40) - (43) and the corresponding forces V and M given by Eqs. (50) and (51), the dynamic stiffness matrix of the Timoshenko beam can be formulated by applying the boundary conditions in algebraic form relating the amplitudes of forces and displacements.

Referring to Fig. 3, the boundary conditions for the displacements and forces can be applied as follows

At $x = 0$ (i.e. $\xi = 0$), $W = \Delta_{y1}$, $\Theta = \Theta_1$, $V = F_{y1}$ and $M = M_1$ (53)

At $x = L$ (i.e. $\xi = 1$), $W = \Delta_{y2}$, $\Theta = \Theta_2$, $V = -F_{y2}$ and $M = -M_2$ (54)

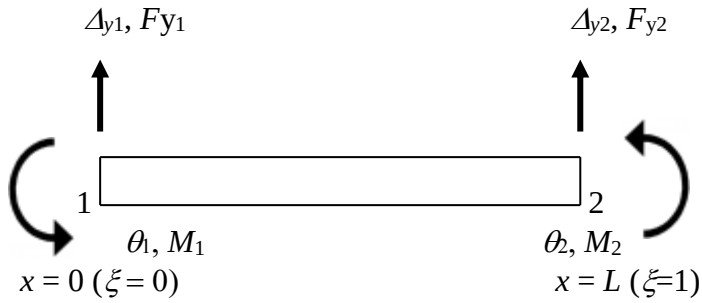

Fig. 3. Boundary conditions for displacements and forces for a Timoshenko beam

Substituting Eqs. (53) and (54) into Eqs. (40)-(43) and Eqs. (50) and (51), the following two matrix equations are obtained for displacements and forces, respectively, in terms of the constants A_1–A_4.

$$\begin{bmatrix}\Delta_{y1}\\ \Theta_1\\ \Delta_{y2}\\ \Theta_2\end{bmatrix} = \begin{bmatrix} 1 & 0 & 1 & 0\\ 0 & k_\Phi/L & 0 & k_\Lambda/L\\ C & S & \bar{C} & \bar{S}\\ -k_\Phi S/L & k_\Phi C/L & jk_\Lambda S/L & k_\Lambda C/L\end{bmatrix}\begin{bmatrix}A_1\\ A_2\\ A_3\\ A_4\end{bmatrix} \quad (55)$$

or

$$\mathbf{\Delta} = \mathbf{Q}\mathrm{A} \quad (56)$$

and

$$\begin{bmatrix} F_{y1} \\ M_1 \\ F_{y2} \\ M_2 \end{bmatrix} = \begin{bmatrix} 0 & -W_3 e_\Phi & 0 & W_3 e_\Lambda \\ W_2 \Phi k_\Phi & 0 & -jW_2 \Lambda k_\Lambda & 0 \\ -W_3 e_\Phi S & W_3 e_\Phi C & -jW_3 e_\Lambda \bar{S} & -W_3 e_\Lambda \bar{C} \\ -W_2 \Phi k_\Phi C & -W_2 \Phi k_\Phi S & jW_2 \Lambda k_\Lambda \bar{C} & jW_2 \Lambda k_\Lambda \bar{S} \end{bmatrix} \begin{bmatrix} A_1 \\ A_2 \\ A_3 \\ A_4 \end{bmatrix} \tag{57}$$

or

$$\mathbf{F} = \mathbf{R}\mathbf{A} \tag{58}$$

where

$$S = \sin\Phi; \quad C = \cos\Phi \tag{59}$$

$$\left.\begin{array}{ll} \bar{S} = \sinh\Lambda; \quad \bar{C} = \cosh\Lambda & b^2 r^2 s^2 < 1 \ \ (j = 1) \\ \bar{S} = \sin\Lambda; \quad \bar{C} = \cos\Lambda & b^2 r^2 s^2 > 1 \ \ (j = -1) \end{array}\right\} \tag{60}$$

and

W_1, W_2 and W_3 are defined as follows

$$W_1 = \frac{EI}{L}; \qquad W_2 = \frac{EI}{L^2}; \qquad W_3 = \frac{EI}{L^3} \tag{61}$$

The constants A_1-A_4 can now be eliminated from Eqs. (55) and (57) to give the 4×4 dynamic stiffness matrix of the Timoshenko beam. This can be achieved by inverting the square matrix of Eq. (55), i.e. **Q** matrix of Eq. (56) and pre-multiplying it with the square matrix of Eq. (57), i.e. **R** matrix and performing the matrix operation $\mathbf{RQ}^{-1}$ numerically to give the dynamic stiffness matrix. Alternatively, the matrix inversion and matrix multiplication procedures can be carried out symbolically (algebraically) to generate explicit expressions for each of the stiffness elements of the dynamic stiffness matrix to give.

$$\begin{bmatrix} F_{y1} \\ M_1 \\ F_{y2} \\ M_2 \end{bmatrix} = \begin{bmatrix} d_1 & d_2 & d_4 & d_5 \\ d_2 & d_3 & -d_5 & d_6 \\ d_4 & d_5 & d_1 & -d_2 \\ -d_5 & d_6 & -d_2 & d_3 \end{bmatrix} \begin{bmatrix} \Delta_{y1} \\ \Theta_1 \\ \Delta_{y2} \\ \Theta_2 \end{bmatrix} \tag{62}$$

where

$$\left.\begin{array}{l} d_1 = W_3 b^2 \Gamma(C\bar{S} + \eta S\bar{C})/(\Lambda\Phi) \\ d_2 = W_2 Z\Gamma\{(\Phi + j\eta\Lambda)S\bar{S} - (\Lambda - \eta\Phi)(1 - C\bar{C})\}/(\Lambda + \eta\Phi) \\ d_3 = W_1\Gamma(S\bar{C} - j\eta C\bar{S}) \\ d_4 = -W_3 b^2 \Gamma(\bar{S} + \eta S)/(\Lambda\Phi) \\ d_5 = W_2 Z\Gamma(\bar{C} - C) \\ d_6 = W_1\Gamma(j\eta\bar{S} - S) \end{array}\right\} \tag{63}$$

with

$$Z = \Phi - b^2 s^2/\Phi; \quad \eta = \mathrm{Z}/(j\Lambda + b^2 s^2/\Lambda);$$
$$\Gamma = (\Lambda + \eta\Phi)/\{2\eta(1 - C\bar{C}) + (1 - j\eta^2)S\bar{S}\} \qquad (64)$$

2.3 Combination of Axial and Bending Stiffnesses

A simple superposition is now possible to put the axial and bending dynamic stiffnesses together in order to express the force-displacement relationship of the combination of a Rayleigh-Love bar and a Timoshenko beam. Superposing Figs. 2 and 3 to give Fig. 4 and then using Eqs. (20) and (62), one obtains the dynamic stiffness matrix of the combination of a Rayleigh-Love bar incorporating the axial stiffnesses, and a Timoshenko beam incorporating the bending stiffness to enable the free vibration analysis of plane frames to be made.

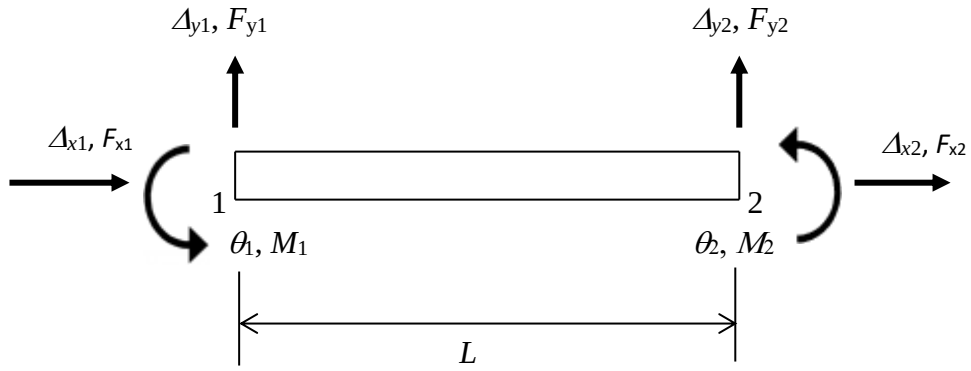

Fig. 4. Amplitudes of displacements and forces at the ends of a combined Rayleigh-Love bar and a Timoshenko beam

Referring to Fig. 4 and Eqs. (20) and (62) the resulting dynamic stiffness matrix is given by

$$\begin{bmatrix} F_{x1} \\ F_{y1} \\ M_1 \\ F_{x2} \\ F_{y2} \\ M_2 \end{bmatrix} = \begin{bmatrix} a_1 & 0 & 0 & a_2 & 0 & 0 \\ 0 & d_1 & d_2 & 0 & d_4 & d_5 \\ 0 & d_2 & d_3 & 0 & -d_5 & d_6 \\ a_2 & 0 & 0 & a_1 & 0 & 0 \\ 0 & d_4 & -d_5 & 0 & d_1 & -d_2 \\ 0 & d_5 & d_6 & 0 & -d_2 & d_3 \end{bmatrix} \begin{bmatrix} \Delta_{x1} \\ \Delta_{y1} \\ \Theta_1 \\ \Delta_{x2} \\ \Delta_{y2} \\ \Theta_2 \end{bmatrix} \qquad (65)$$

or

$$\mathbf{F} = \mathbf{K}\,\boldsymbol{\Delta} \qquad (66)$$

where **F** and **Δ** are respectively the force and displacement vectors and **K** is the frequency dependent 6 × 6 dynamic stiffness matrix whose elements k(i, j) (i = 1,2…6; j = 1,2,…6) are given by a_1, a_2 and d_1-d_6 defined in Eqs. (21) and (63), respectively. Note that **K** is symmetric as expected.

3. Application of the Dynamic Stiffness Matrix

3.1 The Wittrick-Williams Algorithm

The developed dynamic stiffness matrix can now be used to compute the natural frequencies and mode shapes of either an individual Rayleigh-Love bar or a Timoshenko beam or a framework comprising beam elements whose axial stiffnesses are characterized by the Rayleigh-Love bar theory and the bending stiffnesses are characterised by the Timoshenko beam theory. The assembly procedure to obtain the overall dynamic stiffness matrix of the final structure in the global or datum coordinates is similar to the finite element method. For a frame, the standard procedure to create the transformation matrix comprising the sine and cosine of the angle made by the global and local x-axis of each individual bar or beam element are usually used to assemble the overall dynamic stiffness matrix of the frame. A reliable and accurate method of solving the free vibration problem is to apply the Wittrick-Williams algorithm [19] which is well suited for the dynamic stiffness method. The algorithm uses the Sturm sequence property of the dynamic stiffness matrix and ensures that no natural frequencies of the structure analysed are missed. Essentially the algorithm gives the number of natural frequencies that lie below an arbitrarily chosen trial frequency in a straightforward and computationally efficient manner. As successive trial frequencies can be chosen, it is possible to bracket any natural frequency within any desired accuracy.

Before applying the algorithm the dynamic stiffness matrices of all individual elements in a structure are to be assembled to form the overall dynamic stiffness matrix $\boldsymbol{K}_f$ of the final (complete) structure, which may, of course, consist of a single element. The main features of the Wittrick-Williams algorithm and its basic working principles are briefly summarised as follows.

Suppose that ω denotes the circular (or angular) frequency of a vibrating structure, then according to the Wittrick-Williams algorithm [19], j, the number of natural frequencies passed, as ω is increased from zero to ω^*, is given by

$$j = j_0 + \mathrm{s}\{\boldsymbol{K}_f\} \tag{67}$$

where $\boldsymbol{K}_f$, the overall dynamic stiffness matrix of the final structure whose elements all depend on ω, is evaluated at $\omega = \omega^*$; $\mathrm{s}\{\boldsymbol{K}_f\}$ is the number of negative elements on the leading diagonal of $\boldsymbol{K}_f{}^{\Delta}$, $\boldsymbol{K}_f{}^{\Delta}$is the upper triangular matrix obtained by applying the usual form of Gauss elimination to $\boldsymbol{K}_f$, and j_0 is the number of natural frequencies of the structure still lying between

ω=0 and $\omega = \omega^*$when the displacement components to which $\boldsymbol{K}_f$ corresponds are all zeros. (Note that the structure can still have natural frequencies when all its nodes are clamped, because exact member equations allow each individual member to displace between nodes with an infinite number of degrees of freedom, and hence infinite number of natural frequencies between nodes.) Thus

$$j_0 = \sum j_m \tag{68}$$

where j_m is the number of natural frequencies between $\omega = 0$ and $\omega = \omega^*$ for a component member with its ends fully clamped, while the summation extends over all members of the structure. Thus, with the knowledge of Eqs. (67) and (68), it is possible to ascertain how many natural frequencies of a structure lie below an arbitrarily chosen trial frequency. This simple feature of the algorithm (coupled with the fact that successive trial frequencies can be chosen by the user to bracket a natural frequency) can be used to converge on any required natural frequency to any desired (or specified) accuracy.

3.2 The significance of the j_0 count in the Wittrick-Williams algorithm

As explained in section 3.1, one of the requirements for the application of the Wittrick-Williams algorithm is to acquire the needed information about the Clamped-Clamped natural frequencies of individual elements in a structures (the so-called j_0 count) so as to enable the free vibration analysis to be carried out in a flawless and robust manner. However, the determination of the natural frequencies using the Wittrick-Williams algorithm is predominantly based on the sign count s{$\boldsymbol{K}_f$} described in section 3.1. The j_0 count of Eq. (68) is not always needed, particularly if the clamped-clamped natural frequency of none of the constituent members in the structure is exceeded within the frequency range of interest. One way of avoiding the computation of j_0 is to split the structure into large number of elements so that the clamped-clamped natural frequencies of all individual elements become exceptionally high and thus will not be exceeded by any frequency of practical interest. Nevertheless, j_0 count of the algorithm is not really a peripheral issue, particularly for achieving computational efficiency and avoiding further unnecessary discretisation of the structure. The need to compute j_0 stems from the fact that the DSM allows infinite number of natural frequencies to be accounted for when all the nodes of the structure are fully restrained and yet one or more structural members can vibrate freely on their own between the nodes resulting in $\boldsymbol{\delta} = \mathbf{0}$ modes in the eigenvalue equation $[\mathbf{K_D}]\{\delta\} = \mathbf{0}$.

3.3 Clamped-Clamped natural frequencies of a Rayleigh-Love bar

The clamped-clamped natural frequencies of a Rayleigh-Love bar can be obtained from Eqs. (14) and (15) by substituting the boundary conditions of displacements to zero at both ends or alternatively by putting the determinant of the square matrix of Eq. (18) to zero, yielding the frequency equation as

$$\sin\gamma = 0 = \sin n\pi \tag{69}$$

Thus, proceeding in the same way as in the case of classical Bernoulli-Euler bar [16] the number of clamped-clamped natural frequencies j_R of a Rayleigh-Love bar lying below an arbitrarily chosen trial frequency ω^* is given by

$$j_R = \text{highest integer} < \frac{\gamma}{\pi} \tag{70}$$

3.4 Clamped-Clamped natural frequencies of a Timoshenko beam

For a Timoshenko beam, the number of clamped-clamped natural frequencies exceeded by the trial frequency ω^* can be established using the procedure described in [17] to give

$$j_T = j_c - \left[2 - sg\{d_3\} - sg\left\{d_3 - \frac{d_6^2}{d_3}\right\}\right]/2 \tag{71}$$

where sg{ } is +1 or -1 depending on the sign of the quantity within the curly bracket, d_3 and d_6 have already been defined in Eq. (63) and j_c is given by

$$\left.\begin{aligned} j_c &= j_d \quad \text{for } b^2r^2s^2 < 1 \\ j_c &= j_d + j_e \text{ for } b^2r^2s^2 \geq 1 \end{aligned}\right\} \tag{72}$$

with

$$\left.\begin{aligned} j_d &= \text{highest integer} < \frac{\Phi}{\pi} \\ j_e &= \text{highest integer} < \frac{\Lambda}{\pi} + 1 \end{aligned}\right\} \tag{73}$$

In Eq. (73), Φ and Λ have already been defined in Eqs. (44) and (45) respectively. Thus the number of clamped-clamped natural frequencies j_m exceeded by an individual member by the trial frequency ω^* with the inclusion of the Rayleigh-Love bar and the Timoshenko beam theories is given by

$$j_m = j_R + j_T \tag{74}$$

Now the root count j_0 of Eq. (68) can be computed using the Eq. (68) where the summation Σ over m is extended to include all elements in the structure.

4. Results and Discussion

Numerical examples are given for three different types of problems. Example-1 is focused on the natural frequencies of a freely vibrating uniform Rayleigh-Love bar in longitudinal motion with clamped-clamped and cantilever boundary conditions. This is followed by example-2 which is that of a stepped bar taken from the literature. This problem is analysed using both the classical Bernoulli Euler and the Rayleigh-Love theories. Finally example-3 demonstrates the free vibration characteristics of a plane frame for which the dynamic stiffness matrix for each constituent element is based on both Rayleigh-Love and Timoshenko theories as well as classical Bernoulli Euler theories.

4.1 Free longitudinal vibration of a uniform bar

Using the notations given in section 2.1, the natural frequencies of a Rayleigh-Love bar with both ends clamped can be obtained from Eq. (14) by substituting $U(\xi)$ to zero at both $\xi = 0$ and $\xi = 1$ and making appropriate substitution for γ to give the nth natural frequency ω_n as

$$\omega_n = \sqrt{\frac{n^2\pi^2}{\left(1+\frac{\nu^2 I_p n^2\pi^2}{AL^2}\right)}\left(\frac{EA}{\rho AL^2}\right)} \tag{75}$$

where $n = 1, 2, 3, \ldots$.

The corresponding natural frequencies for the classical Bernoulli-Euler with clamped-clamped boundary conditions can be found in standard texts [7] given by

$$\omega_{n_0} = n\pi\sqrt{EA/(\rho AL^2)} \tag{76}$$

The ratio between the natural frequencies for the clamped-clamped bar obtained from the Rayleigh-Love and classical Bernoulli-Euler theories can be expressed with the help of Eqs. (75) and (76) to give

$$\frac{\omega_n}{\omega_{n_0}} = \frac{1}{\sqrt{1+\frac{\nu^2 n^2\pi^2}{\left(\frac{L}{r}\right)^2}}} \tag{77}$$

where r is defined as the radius of gyration expressed as

$$r = \sqrt{\frac{I_p}{A}} \tag{78}$$

Proceeding in a similar way and imposing appropriate boundary conditions, the natural frequency ratio for a cantilever bar using the Rayleigh-Love and classical Bernoulli-Euler theories can be expressed as

$$\frac{\omega_n}{\omega_{n_0}} = \frac{1}{\sqrt{1+\frac{(2n-1)^2\pi^2\nu^2}{4\left(\frac{L}{r}\right)^2}}} \tag{79}$$

The validity of the Eqs. (77) and (79) has been further confirmed by using the developed dynamic stiffness matrix of a Rayleigh-Love bar shown in Eq. (20).

Clearly Eqs. (77) and (79) indicate that the natural frequency ratio $\frac{\omega_n}{\omega_{n_0}}$ is dependent on the Poisson's ratio ν of the bar material as well as the slenderness ratio *L/r* of the bar. The Poisson's ratio ν for an isotropic material is generally constant and maybe assumed to be 0.3 which is used here in the analysis.

Figures. 5 and 6 show the variation of the ratio of the first five natural frequencies using the Rayleigh-Love and classical Bernoulli-Euler theories against the slenderness ratio *L/r* for the clamped-clamped and cantilever bar respectively. Clearly for smaller values of slenderness ratios and for higher natural frequencies, the classical Bernoulli-Euler theory is considerably less accurate. The errors incurred in the fifth natural frequency when using the classical Bernoulli-Euler theory are 27% and 24% for the clamped-clamped and cantilever bar respectively when the slenderness ratio is 5. It should be noted that in the Statistical Energy Analysis (SEA) for which modal density in the high frequency range is required, the classical Bernoulli-Euler theory can be inadequate.

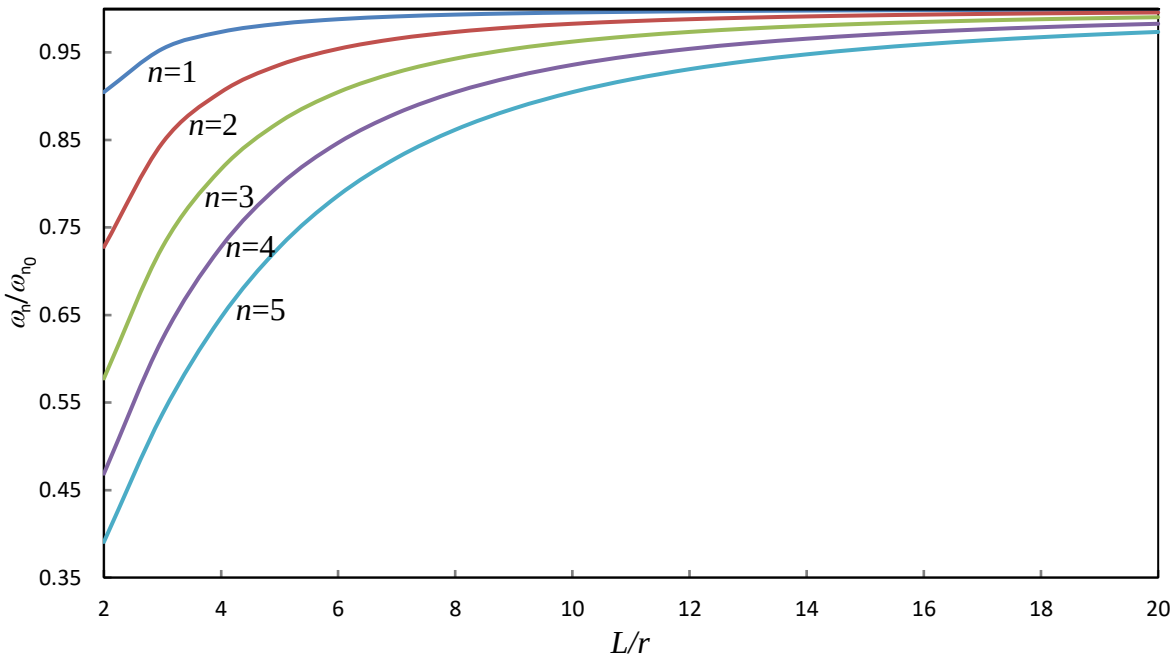

Fig. 5. The first five natural frequency ratios using the Rayleigh-Love and classical Bernoulli-Euler theories for a clamped-clamped bar. ω_n = natural frequency using Rayleigh-Love theory; ω_{n0} = natural frequency using classical Bernoulli-Euler theory.

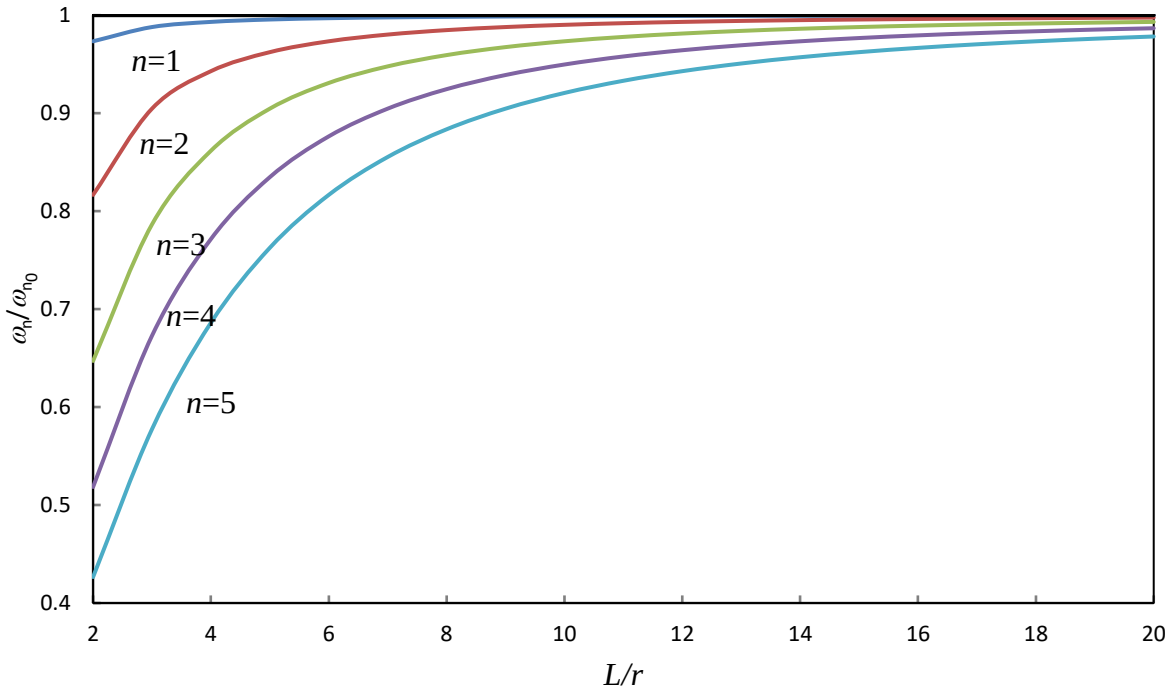

Fig. 6. The first five natural frequency ratios using the Rayleigh-Love and classical Bernoulli-Euler theories for a cantilever bar. ω_n = natural frequency using Rayleigh-Love theory; ω_{n0} = natural frequency using classical Bernoulli-Euler theory.

4.2 Free longitudinal vibration of a stepped bar

A stepped bar (example-2) which is taken from [34] and shown in Fig. 7. is analysed for its free vibration characteristics in longitudinal motion using the developed dynamic stiffness matrix. The stepped bar is cantilevered at the left hand end as shown and consists of three individual bars of solid circular cross-section with different geometrical dimensions and material properties for each. The essential data required for the analysis are: radius of cross-section (r_i), length (l_i), Young's modulus (E_i), density (ρ_i) and Poisson's ratio (ν_i) (i representing the segment or element number).

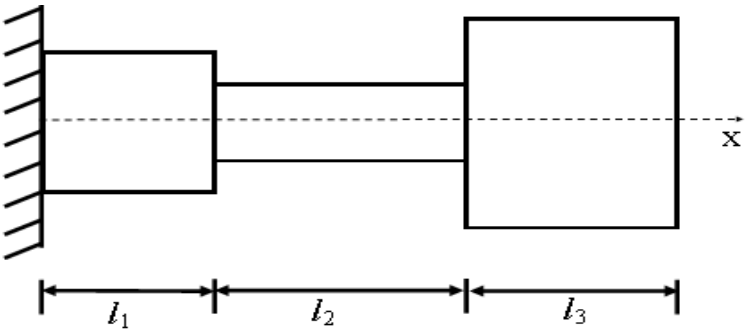

Fig. 7. A three-stepped bar for free vibration analysis.

The numerical values for the data taken from [34] are:

r_1 = 0.05m, r_2 = 0.03m, r_3 = 0.075m,

l_1 = 0.05m, l_2 = 0.17m, l_3 = 0.13m,

E_1 = 200×10^9 Pa, E_2 = 70×10^9 Pa, E_3=100×10^9 Pa,

ρ_1 = 7.85×103 kg/m^3, ρ_2 = 2.7×103 kg/m^3, ρ_3 = 8.4×103 kg/m^3,

ν_1 = 0.30, ν_2 = 0.33, ν_3 = 0.34.

The first four natural frequencies computed using the Rayleigh-Love dynamic stiffness theory are shown in column 2 of Table1 alongside the results reported in [34] shown in column 3. The corresponding natural frequencies computed using classical Bernoulli-Euler dynamic stiffness theory [16] are also shown in the parenthesis in column 2. Although the agreement of the results between the present theory and those of [34] are good for the second and fourth natural frequencies (the differences are well within 3%), but for the first and third natural frequencies there are some discrepancies which are around 13% and 15% respectively. The fundamental natural frequency of the bar quoted in [34] is well above the corresponding natural frequency obtained from the classical Bernoulli-Euler theory. This is surely in error because the effect of the transverse inertia presumably accounted for in [34] is expected to diminish the natural frequency and not increase it. The mode shapes corresponding to the four natural frequencies using the present theory are shown in Fig. 8 by solid lines which are in broad agreement with the ones reported in [34]. The mode shapes shown by dash lines are those computed using the classical Bernoulli-Euler theory. Clearly, the first three mode shapes have undergone very little changes as a result of using the present theory as opposed to the classical Bernoulli-Euler theory, but the fourth mode being a higher order mode has turned out to be significantly different, as expected. The authors were unable to pinpoint the exact reason for the discrepancies in the first and third natural frequencies, when they compared their results with those of [34], but it should be recognised that the series solution approach used in [34] is different from the dynamic stiffness methodology developed in this paper. It is to be noted that both the Rayleigh-Love and the classical Bernoulli-Euler theories give almost the same results for the fundamental natural frequency, but the differences in the second, third and fourth frequencies are 7%, 4% and 21% respectively. Understandably, the classical Bernoulli-Euler theory overestimates the natural frequencies whereas the more refined Rayleigh-Love theory which accounts for the added transverse and lateral inertia of the bar yields lower values of the natural frequencies which is apparently contradicted by the result for the fundamental natural frequency reported in [34].

Table 1: Natural frequencies of a stepped bar in longitudinal vibration (results from the conventional classical theory are shown in the parenthesis in column 2).

Frequency Number	Natural Frequency (*Hz*)	
	Current Theory	Ref. [34]
1	1184.312 (1184.39)	1362.79
2	11732.86 (12509.42)	11679.6
3	14503.42 (15002.56)	12640.5
4	20014.45 (24187.29)	19461.9

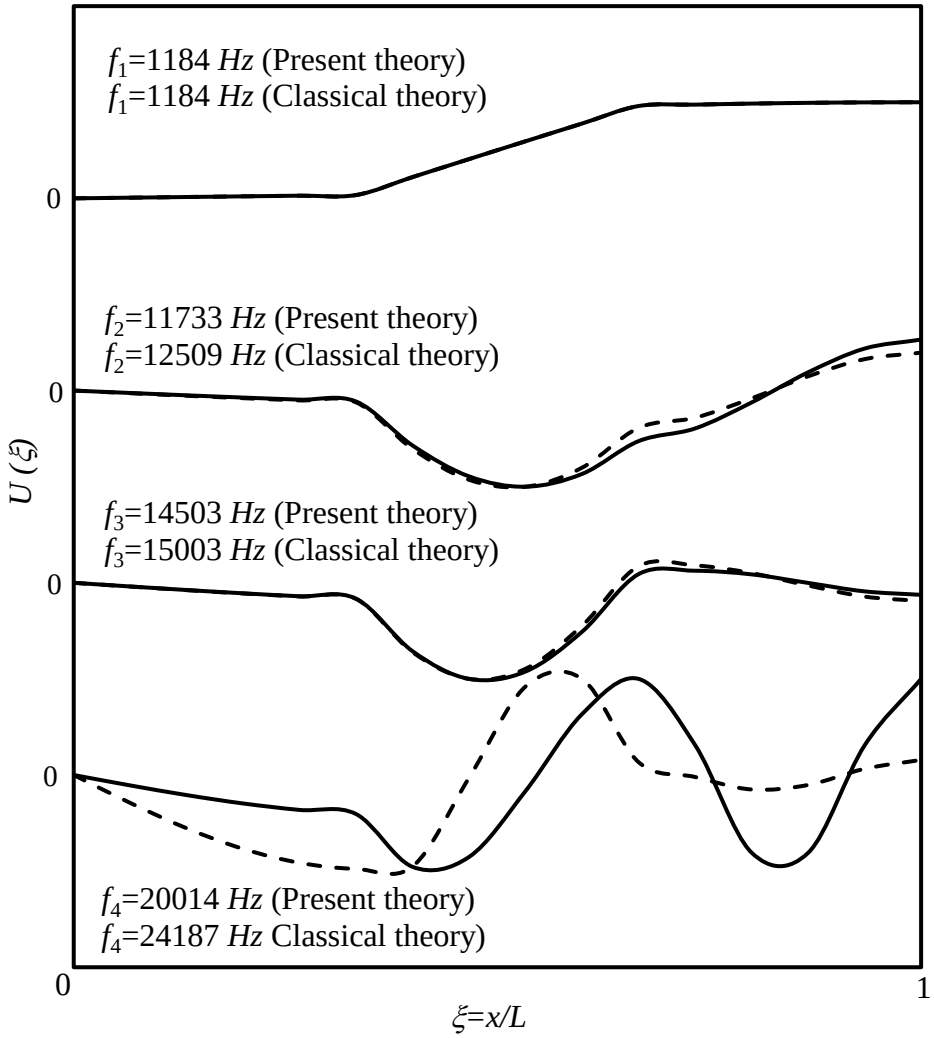

Fig. 8. Natural frequencies and mode shapes of the three-stepped bar of Fig 7.

——————— Present theory; ---------- Classical theory.

4.3 Free vibration of a plane frame

The final set of results was obtained using example-3 which is that of a plane frame shown in Fig. 9. Each element of the frame has the same uniform geometrical, cross sectional and material properties and the data used in the analysis are as follows:

$EI = 4.0\times10^{6}$ Nm^2, $EA = 8.0\times10^{8}$ N, $kAG = 2.0\times10^{8}$ N,

$\rho A = 30$ kg/m, $\rho I_p = 0.157$ kgm, $\nu = 1/3$, $k = 2/3$

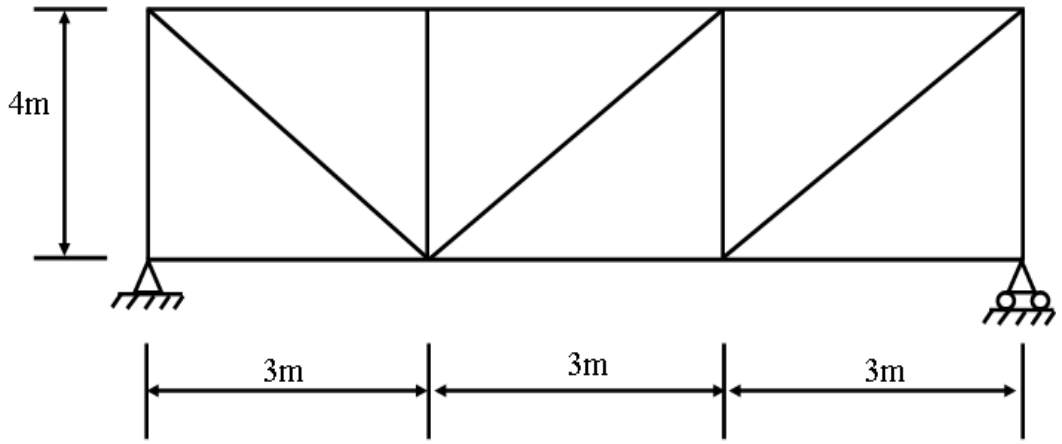

Fig. 9. A plane frame for free vibration analysis using Rayleigh-Love and Timoshenko theories.

A wide range of the natural frequencies of the frame was computed using the present theory as well as the classical Bernoulli-Euler theory. Apart from the computation of the first five natural frequencies which were sequentially chosen, the higher order natural frequencies were sparingly and sparsely chosen so as to cover the order of the natural frequencies between 50th and 400th. The results are shown in Table 2. Clearly, higher the order of the frequency, higher the incurred error due to using the classical Bernoulli-Euler theory. The first five natural frequencies of the frame are virtually unaltered. As expected, the classical Bernoulli-Euler theory overestimates the natural frequencies.

Table 2: Natural frequencies of plane frame

Frequency Range	Natural Frequency Number (i)	Natural Frequency f_i (Hz)	
		Rayleigh-Love and Timoshenko theory	Classical Bernoulli-Euler theory
Low	1	35.38	35.77
	2	38.56	39.10
	3	41.98	42.56
	4	50.73	51.39
	5	53.14	53.94
Medium	50	565.54	600.97
	60	635.28	709.09
	70	828.95	934.39
	80	964.48	1136.00
	90	1108.90	1301.20
	100	1306.80	1521.40
High	150	2151.10	2732.30
	200	3047.50	4089.50
	250	3940.30	5585.00
	300	4859.70	7152.20
	350	5767.40	8744.80
	400	6112.80	10495.00

One of the potential application areas of the theory developed in this paper is the Statistical Energy Analysis (SEA) for which accurate natural frequency predictions in the low, medium and high frequency range are essential. To this end, the uncompromising accuracy of the dynamic stiffness method developed in this paper by applying the Rayleigh-Love and Timoshenko theories is further demonstrated by computing the number of natural frequencies of the frame (see Fig. 10) which lies within the frequency ranges of $0 < f_i \leq 1kHz$, $0 < f_i \leq 2kHz$, $0 < f_i \leq 3kHz$ and up to $0 < f_i \leq 10kHz$ which cover low, medium and high frequency bands. Figure 10 shows the frequency distribution, i.e. the modal density of the frame. It will be difficult to obtain these results with such accuracy using conventional Finite Element Method.

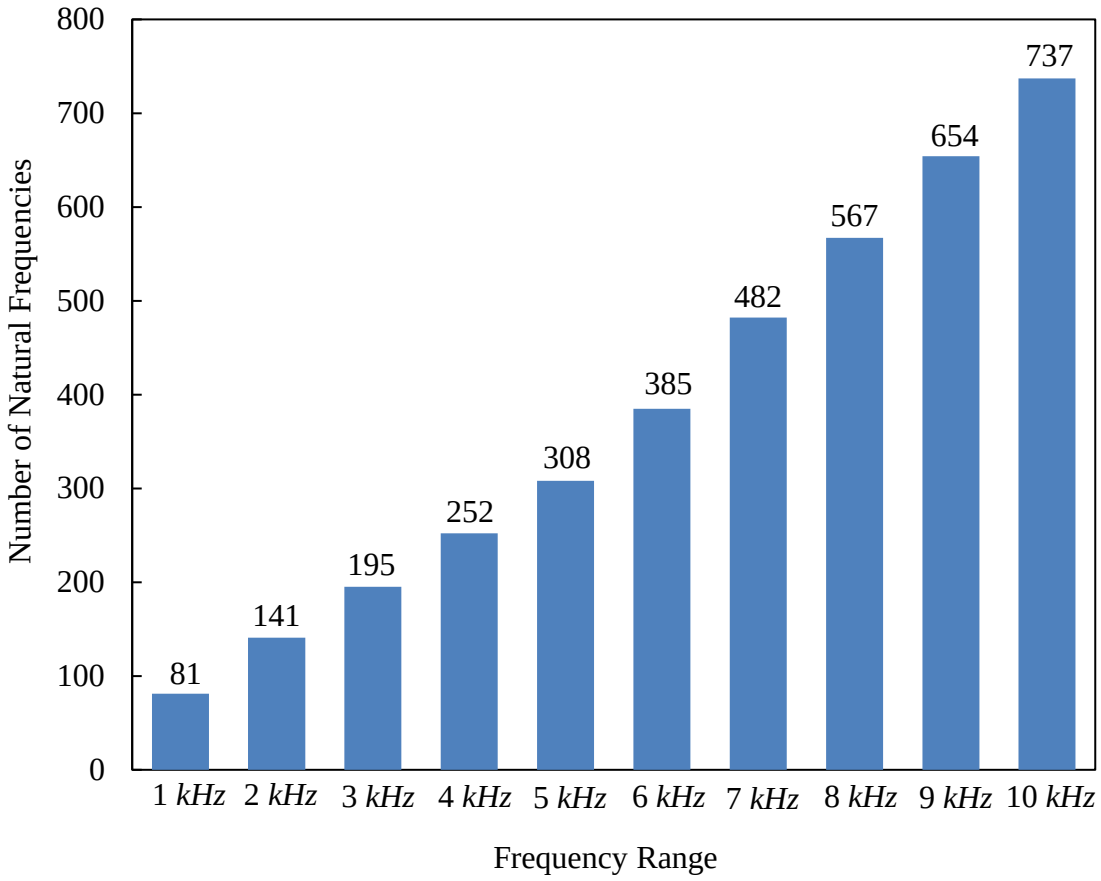

Fig. 10. Modal density of plane frame.

5. Limitations and Scope for Further Developments of the Theory

The dynamic stiffness theory presented in this paper deals with Rayleigh-Love bars and Timoshenko beams made of homogenous and isotropic materials for which the essential properties are Young's modulus (E), shear modulus (G), Poisson's ratio (ν) and density (ρ). Further development of the theory and its future applications to include laminated composites will be a challenge, and indeed, a major task mainly because of the fibrous nature of such anisotropic materials, which require more elastic constants to define their properties. Also the introduction of a fictitious shape factor or shear correction factor as demanded by the assumption in the Timoshenko beam theory to account for the non-uniform shear stress distribution through the thickness of the beam cross-section, is no-doubt a limitation. In this respect, the current theory can be extended by incorporating higher order shear deformation theories [35, 36] in the analysis. To overcome the limitations of the theory presented in this paper, particularly for its extension to anisotropic fibrous composites, interested readers are referred to the review papers of Sayyad and Ghugal [37, 38] for necessary background information.

6. Conclusions

Starting from the derivations of the governing differential equations of motion in free vibration, the dynamic stiffness matrix of a beam using both the Rayleigh-Love and Timoshenko theories has been developed. With the help of the Wittrick-Williams algorithm as solution technique, the theory is applied to investigate the free vibration behaviour of a uniform Rayleigh-Love bar, a stepped Rayleigh-Love bar, and a framework for which the modal density distribution is presented by capturing its natural frequencies in the low, medium and high frequency range. Some representative mode shapes of the stepped bar are also illustrated. The theory developed is particularly helpful when carrying out high frequency free vibration analysis of skeletal structures. A potential application of the research described in this paper falls within the area of statistical energy analysis for which the knowledge of modal density distributions in the high frequency range is essential.

Acknowledgements

The authors are grateful to Dr Alfonso Pagani of the Polytechnic University of Turin, Italy and Dr William Tiu of BA Systems, UK for many stimulating email exchanges on the subject. Also the first author benefitted from a related past EPSRC(UK) project (Grant Ref GR/R21875/01) to whom acknowledgement is hereby made.

References

[1] Keane AJ, Price WC. Statistical energy analysis: An overview, with applications in structural dynamics. Cambridge University Press; 1997.

[2] Lyon RH, DeJong RG. Theory and application of statistical energy analysis, second edition. Butterworth-Heinermann; London, 1995.

[3] Wohlever JC, Bernhard RJ. Mechanical energy flow models of rods and beams. J Sound Vib 1992;153:1–19. doi:10.1016/0022-460X(92)90623-6.

[4] Lase Y, Ichchou MN, Jezequel L. Energy flow analysis of bars and beams: Theoretical formulations. J Sound Vib 1996;192:281–305. doi:10.1006/jsvi.1996.0188.

[5] Bouthier OM, Bernhard RJ, Laboratories H, Lafayette W. Simple models of energy flow in vibrating membranes. J Sound Vib 1995;182:129–47. doi:10.1006/jsvi.1995.0186.

[6] Bouthier OM, Bernhard RJ. Simple models of the energetics of transversely vibrating plates. J Sound Vib 1995;182:149–64. doi:10.1006/jsvi.1995.0187.

[7] Rao SS. Vibration of continuous systems, first edition. John Wiley & Sons; 2007.

[8] Leissa AW, Qatu MS. Vibration of continuous systems, first edition. McGraw-Hill Education; 2011.

[9] Meirovitch L. Fundamentals of vibrations, first edition. Waveland Pr Inc; 2010.

[10] Thomson WT. Theory of vibration with applications, fourth edition. CRC Press; 1996.

[11] Chopra AK. Dynamics of structures: theory and applications to earthquake engineering, fourth edition. Pearson; 2015.

[12] Koloušek V. Anwendung des gesetzes der virtuellen verschiebungen und des reziprozitätssatzes in der stabwerksdynamik. Ingenieur-Archiv 1941;12:363–70. doi:10.1007/BF02089894.

[13] Koloušek V. Berechnung der schwingenden stockwerkrahmen nach der deformationsmethode. Der Stahlbau 1943;16:11-13.

[14] Koloušek V. Dynamics in engineering structures. Newnes-Butterworth; 1973.

[15] Åkesson B. PFVIBAT—a computer program for plane frame vibration analysis by an exact method. Int J Numer Methods Eng 1976;10:1221–31. doi:10.1002/nme.1620100603.

[16] Williams FW, Howson WP. Compact computation of natural frequencies and buckling loads for plane frames. Int J Numer Methods Eng 1977;11:1067–81. doi:10.1002/nme.1620110704.

[17] Howson WP, Banerjee JR, Williams FW. Concise equations and program for exact eigensolution of plane frames including member shear. Advances in Engineering Software 1983;5:137-41.

[18] Banerjee JR. Dynamic stiffness formulation for structural elements: A general approach. Comput Struct 1997;63:101–3. doi:10.1016/S0045-7949(96)00326-4.

[19] Wittrick WH, Williams FW. A general algorithm for computing natural frequencies of elastic structures. Q J Mech Appl Math 1971;24:263–84.

[20] Han JB, Hong SY, Song JH, Kwon HW. Vibrational energy flow models for the Rayleigh-Love and Rayleigh-Bishop rods. J Sound Vib 2014;333:520–40. doi:10.1016/j.jsv.2013.08.027.

[21] Shatalov M, Marais J, Fedotov I, Tenkam MJ. Longitudinal vibration of isotropic solid rods: from classical to modern theories. 2011. doi: 10.5772/15662.

[22] Lord Rayleigh. The theory of sound: vol. 1-2. Cambridge University Press; 2011.

[23] Love A.E.H. A treatise on the mathematical theory of elasticity, fourth edition. Cambridge University Press; 2013.

[24] Belov VD, Rybak SA, Tartakovskii BD. Propagation of vibrational energy in absorbing structures. Journal of Soviet Physics Acoustics 1977; 23:115-19.

[25] Nefske DJ, Sung SH. Power flow finite element analysis of dynamic systems: Basic theory and application to beams. J Vib Acoust Stress Reliab Des 1989;111:94–100. doi:10.1115/1.3269830.

[26] Lase Y, Ichchou MN, Jezequel L. Energy flow analysis of bars and beams: theoretical formulations. J Sound Vib 1996;192:281-305.

[27] Cheng FY. Vibration of Timoshenko beams and frameworks. J. Struct. Div, ASCE 1970; 96:551-71.

[28] Wang TM, Kinsman TA. Vibration of frame structures according to the Timoshenko theory. J Sound Vib 1971;14:215-27.

[29] Howson WP, Williams FW. Natural frequencies of frames with axially loaded Timoshenko members. J Sound Vib 1973;26:503-15.

[30] Wang T M, Kinsman TA. Vibration of frame structures according to the Timoshenko theory. J Sound Vib 1971; 14:215-27.

[31] Banerjee, J.R., Sobey, A.J., Su, H., and Fitch, J.P. Use of computer algebra in Hamiltonian calculations. Adv Eng Software, 2008;39(6):521-525.

[32] Predoi MV, Petre CC, Vasile O, Boiangiu M. High frequency longitudinal damped vibrations of a cylindrical ultrasonic transducer. Shock Vib 2014. doi:10.1155/2014/105971.

[33] Hurty WC, Rubinstein MF. Dynamics of Structures. Prentice Hall; 1964.

[34] Fedotov I, Gai Y, Polyanin A, Shatalov M. Analysis for an N-stepped Rayleigh bar with sections of complex geometry. Appl Math Model 2008;32:1–11. doi:10.1016/j.apm.2006.10.028.

[35] Heyliger PR, Reddy JN. A higher order beam finite element for bending and vibration problems. J Sound Vib 1988;126:309–26. doi:10.1016/0022-460X(88)90244-1.

[36] Eisenberger M. Dynamic stiffness vibration analysis using a high-order beam model. Int J Numer Methods Eng 2003;57:1603–14. doi:10.1002/nme.736.

[37] Sayyad AS, Ghugal YM. On the free vibration analysis of laminated composite and sandwich plates: A review of recent literature with some numerical results. Compos Struct 2015;129:177–201. doi:10.1016/j.compstruct.2015.04.007.

[38] Sayyad AS, Ghugal YM. Bending, buckling and free vibration of laminated composite and sandwich beams: A critical review of literature. Compos Struct 2017;171:486–504. doi:10.1016/j.compstruct.2017.03.053.